Basic Research in Cardiology (2019) 114:40
https://doi.org/10.1007/s00395-019-0748-8

ORIGINAL CONTRIBUTION

Connexin 43 dephosphorylation contributes to arrhythmias and cardiomyocyte apoptosis in ischemia/reperfusion hearts

Jingyi Xue[1] · Xinxin Yan[1,2] · Yutong Yang[1] · Min Chen[1] · Lulin Wu[1] · Zhongshan Gou[1,2] · Zhipeng Sun[1] · Shaletanati Talabieke[1] · Yuanyuan Zheng[1] · Dali Luo[1]

Received: 8 May 2019 / Accepted: 19 August 2019 / Published online: 28 August 2019

Abstract

Connexin 43 (Cx43)-associated gap junctions form electrical and mechanical conduits between adjacent ventricular cardiomyocytes, ensuring coordinate electrical excitation and synchronic contraction for each heartbeat. Cx43 dephosphorylation is a characteristic of ischemia, arrhythmia, and a failing and aging myocardium, but the exact phosphosite(s) triggering myocardial apoptosis and electrical disturbance and its underlying mechanisms are unclear. We previously found that Cx43-serine 282 phosphorylation (pS282) can regulate cardiomyocyte survival and electrical stability. Here, we investigated the hypothesis that S282 dephosphorylation occurs in and contributes to ischemia/reperfusion (*I*/*R*)-induced cardiac injury. We found enhanced Cx43-pS262 and Cx43-pS368 but decreased Cx43-pS282 in rat hearts subjected to *I*/*R* (30 min/2 h). *I*/*R* rats had ventricular arrhythmias and myocardial apoptosis with activation of the p38 mitogen-activated protein kinase (p38)/factor-associated suicide (Fas)/Fas-associating protein with a novel death domain (FADD) pathway. Similarly, S282 dephosphorylation, abnormal Ca^{2+} transients, cell apoptosis and p38/Fas/FADD activation also occurred in neonatal rat ventricular myocytes exposed to anoxia/reoxygenation (12/6 h). To confirm the causative role of S282 dephosphorylation in cardiac injury, rat hearts were intramyocardially injected with a virus carrying the S282 mutant substituted with alanine (S282A), thus causing arrhythmias and reducing cardiac output and myocardial apoptosis with p38/Fas/FADD pathway activation. Moreover, Cx43-S282A$^{+/-}$ mice displayed arrhythmias and impaired cardiac output with global myocardial apoptosis. Our findings revealed that Cx43 dephosphorylation at S282 triggers arrhythmias and, at least partly, contributes to cardiomyocyte death upon *I*/*R* by activating the p38/Fas/FADD pathway, providing a novel molecular mechanism and potential target for protecting against cardiac *I*/*R* injury.

Keywords Connexin 43 · Phosphorylation · Ischemia/reperfusion · Apoptosis · Arrhythmia

Introduction

Myocardial ischemia is the leading cause of lethal cardiac diseases worldwide due to life-threatening arrhythmias and myocardial infarction. Paradoxically, the major therapeutic strategy targeting blood flow recovery to the ischemic area may facilitate myocardial injury and dysfunction if performed improperly. This is known as ischemia/reperfusion (*I*/*R*) injury and contributes significantly to cardiac infarction morbidity and mortality [9, 10, 15, 43]. Myocardial apoptosis and necrosis are the fundamental pathological processes for acute *I*/*R*-induced cardiac injury, and several stimuli, including reactive oxygen species generation, autoimmune response and excess ATP consumption, have been proposed to activate the cardiomyocyte death machinery [2, 8, 15, 37]. In addition, alterations in connexin 43 (Cx43)

Electronic supplementary material The online version of this article (https://doi.org/10.1007/s00395-019-0748-8) contains supplementary material, which is available to authorized users.

Jingyi Xue, Xinxin Yan and Yutong Yang contributed equally to this work.

✉ Dali Luo
luodl@ccmu.edu.cn

[1] Department of Pharmacology, Beijing Key Laboratory of Metabolic Disturbance Related Cardiovascular Disease, School of Basic Medical Sciences, Capital Medical University, District of Fengtai, Street of Youanmenwai, #10 Xitoutiao, Beijing 100069, People's Republic of China

[2] Present Address: The Affiliated Suzhou Hospital of Nanjing Medical University, Suzhou 215008, Jiangsu, People's Republic of China

phosphorylation, the predominant ventricular gap channel protein, have been implicated to play a profound role in severe myocardial lesions [9, 10, 31, 48].

More than ten serine residues in the Cx43 carboxyl terminus (Cx43-CT), a substrate of several kinases, are highly phosphorylated in normal myocardium and are essential for synchronizing cardiac functional performances and maintaining cardiomyocyte homeostasis [11, 24, 49]. Under pathological conditions, Cx43 is dephosphorylated by mostly undefined mechanisms, which is a characteristic event in ischemia and nonischemic heart diseases across species, including myocardial ischemia, arrhythmias, diabetes, and aging and failing hearts [9, 10, 24, 31, 49]. Specific dephosphorylated serines, including serine 325 (S325)/328/330 [3, 27, 39], S365 [51], S368 [52] and S297 [13], are found in ischemic and *I*/*R* hearts. Mimicking S262, S368 or S325/328/330 dephosphorylation renders cardiomyocytes susceptible to ischemic death and electrical instability under detrimental stimuli [3, 13, 24, 27, 39], while enhanced phosphorylation at S368 or S262 found at the beginning of (S368) and during (S373 and S262) cardiac ischemia contributes to cytoprotection against ischemic injury [13, 24, 27, 29, 36, 51, 52]. Therefore, regulating Cx43-CT phosphorylation in the heart during *I*/*R* is twofold. First, dephosphorylation at specific serine residues inhibits the injured signal to propagate to the adjacent cardiomyocytes [18, 34, 46] while simultaneously sensitizing the heart to apoptosis and electrical disturbances to stress stimulation [3, 13, 24, 27, 34, 36, 51, 52]. Second, increased phosphorylation at specific serines protects cardiomyocytes from *I*/*R* injury, which provides an emerging therapeutic target for severe heart diseases [3, 24, 34, 36, 46, 55]. All data obtained thus far indicate that modifying Cx43 phosphorylation plays an important role in generating cardiomyocyte death and electrical disorders in severe heart diseases. However, which Cx43-phosphosite(s) directly trigger disorders in cardiomyocyte electrical activity and survival status and which are relevant to the pathophysiology in injured heart diseases remain unclear.

In a previous study, we found spontaneous arrhythmias and myocardial apoptosis in heterozygous mice with a Cx43 mutation at S282 by alanine ($S282A^{+/-}$, to deprive S282 phosphorylation) in a pS282-deficiency-dependent fashion as well as abnormal Ca^{2+} transients and cell death in primary cultured neonatal rat ventricular myocytes (NRVMs) transfected with S282A under basal conditions [57]. Coexpression of wild-type Cx43 (Cx43-wt) or a mutant substitute with aspartate (S282 phospho-mimic) could not rescue the disturbed Ca^{2+} signals and lethal effect of S282A in the NRVMs, indicating a dominant negative effect. In addition, dramatic p38 mitogen-activated protein kinase (p38) phosphorylation and enhanced expressions of factor-associated suicide (Fas) and Fas-associating protein with a novel death domain (FADD) were involved in the deficient S282 phosphorylation-induced cell apoptosis in both in vitro and in vivo studies. These results suggest an intrinsic regulatory role of pS282 in physiologic cardiomyocyte survival and electrical stability [57]. Thus, in this study, we investigated the pathological effect of S282 phosphorylation during *I*/*R*-induced myocardial injury. We found significant S282 dephosphorylation and p38/Fas/FADD pathway activation in *I*/*R* rat hearts and anoxia/reoxygenation (*A*/*R*)-treated NRVMs. Further evaluating rats with ventricles subjected to local S282A transfection, we found ventricular arrhythmias, decreased cardiac output and local myocardial apoptosis and injury, mimicking *I*/*R* heart manifestations. Heterozygous mouse hearts with an $S282A^{+/-}$ mutant also displayed S282-dephosphorylation-dependent animal death, arrhythmias, cardiac dysfunction and myocardial apoptosis. These data support our hypothesis that Cx43 dephosphorylation at S282 occurs during *I*/*R* and is involved in triggering myocardial apoptosis and electrical disability, providing a novel molecular mechanism underpinning Cx43 involvement in inducing *I*/*R*-related heart injury.

Materials and methods

Animals

Animals were maintained in the Center for Experimental Animals at Capital Medical University (Beijing, China), and kept on a 12-h light–dark cycle in a temperature-controlled room with ad lib access to food and water. All the animal experiments in this study were approved by the Capital Medical University Animal Care and Use Committee (AEEI-2015-193) and conducted in accordance with the "Guide for the Care and Use of Laboratory Animals" adopted by Beijing Municipal People's Government and the National Institutes of Health's Guidance.

Cardiac ischemia/reperfusion model

I/*R* injury was performed in sixty Sprague–Dawley male rats (12–13 weeks old) obtained from the Center of Experimental Animal at Capital Medical University (Beijing, China) as previously described [17]. Briefly, rats were anesthetized intraperitoneally with pentobarbital (100 mg/kg). The left chest was opened to expose the heart and an 8–0 silk suture was passed underneath the left anterior descending coronary artery (LAD), and then tied a slipknot. The rats were subjected to 30-min ligation followed by 2 h of reperfusion (Supplementary Fig. 1). Significant elevations of S–T segment detected by surface electrocardiograph (ECG) indicated a successful operation in these rats. Sham-operated rats underwent the same procedures except that the suture was placed beneath the LAD without ligation.

To determine the infarct area (IA) and area at risk (AAR), the LAD was reoccluded and 2 ml of 2% Evans blue dye (Sigma) was injected into the left ventricular cavity after *I/R* injury. The heart was quickly removed, frozen at − 80 °C and sliced horizontally to yield fives slices. The heart slices were incubated in 1.0% 2,3,5-triphenyltetrazolium chloride (TTC, Sigma) prepared with phosphate buffer (pH 7.8) for 15 min at 37 °C, and fixed in 10% neutral buffered formaldehyde. Both sides of each slice were photographed using Lumar V12 Stereomicroscope (ZEISS). The IA (TTC-negative area), AAR (TTC-positive area) and total left ventricular area (LV) were analyzed by planimetry with ImageJ (http://imagej.nih.gov/ij/). The infarct size was then expressed as a percentage of the AAR or LV area.

To determine the lactate dehydrogenase (LDH) and cardiac troponin-I (cTn-I) release for indication of cardiomyocyte damage, the blood outflows of heart immediately after *I/R* were used. Blood samples were collected and centrifuged for 10 min at 3000 rpm to obtain serum. LDH and cTn-I were spectrophotometrically assayed using LDH and cTn-I kits (Sigma) according to the manufacturer's instructions.

Anoxia and reoxygenation model

NRVM isolation and culture were performed as previously described [26, 30]. After cultured for 6 h in the absence of fetal bovine serum, NRVMs were exposed to anoxia followed by reoxygenation (*A/R*) treatment as previously described [26]. Briefly, cardiomyocytes were exposed to anoxia in serum-free DMEM with vehicle control, 58 nM cantharidinate (CA, MilliporeSigma, USA), and incubated in an anoxic chamber (Thermo3100, USA) with an atmosphere of 95% N_2 and 5% CO_2 for 12 h. Cells were returned to reoxygenation medium and incubated in an incubator with an atmosphere of 95% O_2 and 5% CO_2 for 6 h, while cells in control normoxia experiments were incubated in fresh culture medium in an incubator with 95% O_2 and 5% CO_2 for 18 h.

Adenovirus constitution

Recombinant plasmids and adenoviral vectors carrying wild-type Cx43 (*Cx43-wt*) or Cx43 S282 substituted with alanine (*S282A*) genes were constructed as previously described [25].

Intramyocardial injection of virus

Sprague–Dawley male rats (250 ± 20 g, $n = 50$) were divided into three groups. After anesthetized with pentobarbital (100 mg/kg), rats were injected with adenovirus constructs of vector, Cx43-wt and S282A into the anterior wall of the left ventricle under ultrasound image guidance as previously described [42]. Virus constructs were diluted with 0.9% saline to a final concentration of 1×10^9 virus particles in 100 µl. Briefly, a 30-gauge needle in a 50-µl syringe was used. The needle was penetrated through the chest to left ventricle chamber, and then went back until the needle reached the injection position in the left ventricle wall, where viruses were injected over a period of 5–7 s. Altogether four injections (25 µl for each site) into the anterior wall of rat heart were performed in a sequent sites A–D as the plot indicated (Fig. 5a). Surface ECG was monitored twice a day. On the fifth day post-injection, S282A animals displayed significant changes in ECG measurements, and all the animals were subjected to anesthesia for examination of ultrasonic cardiogram (UCG) and then hearts were taken for further examinations (Supplementary Fig. 1).

Generation of Gja1 S282A mutant mice

S282A mutant mice were generated, and experiments on these mice were performed as previously described [57].

Echocardiography and electrocardiograph

Rats and mice were intubated and anaesthetized with mechanical ventilation by inhalation of 1–1.5% isoflurane (RWD, Batch) in 100% oxygen continuously. Body temperature was maintained by a heating pad. M-mode echocardiography was performed using a high-resolution ultrasound system (VisualSonics Vevo 770, Toronto, Canada) equipped with a frequency transducer (frequency band 12–38 MHz). Left ventricular anterior/posterior wall thickness (LVAW/LVPW) and parameters of ejection fraction (EF) and fraction shortening (FS) were measured and calculated by VisualSonics analysis software (version 2.1.0) from the average of five beats.

Surface ECG was monitored using P3 Plus (Data Sciences International) for every animal anaesthetized by a 1.5% isoflurane oxygen mixture with sub-dermal platinum electrodes placed in lead II arrangement. Body temperature was maintained at 37 °C. An ECG sample of 3 min of each animal was analyzed. Time intervals, S–T section and QRS-time were measured from the mean curve of 1 min with a specially made LabChart7 analysis program. ECG recording was marked at 30 min after rat ligation and 1 h after reperfusion for *I/R* rats and twice a day for virus-injected rats and S282 mutation mice. Ventricular tachycardia (VT) was defined as at least four consecutive premature ventricular beats (PVB).

Mitochondrial isolation

Mitochondria/cytosol fractionation kit (Beyotime Int. Biotech, Peking, China) was used to isolate subcellular

cytoplasmic and mitochondrial fractionations according to instruction. Briefly, NRVMs were collected and washed in PBS. Then the cells in mitochondrial isolation buffer with 1 mM phenylmethylsulfonyl fluoride (PMSF) were lysed on ice for 15 min and homogenized for 10–20 strokes. The homogenate was centrifuged at 600×*g* for 10 min at 4 °C, and the supernatant was collected and centrifuged at 3500×*g* for 10 min at 4 °C. After addiction of mitochondrial lysate with 1 mM PMSF, the substratum was used as the mitochondrial fraction, and supernatants were centrifuged at 12,000 rpm for 10 min at 4 °C. Then the supernatant was used for the analysis of cytosolic fraction. GAPDH and Cox-IV were used as reference for cytosolic and mitochondrial fractions, respectively.

Assessment of apoptosis

Apoptosis evaluations in NRVMs and heart tissue were performed by Annexin V-FITC/PI staining using flow cytometry and terminal deoxyribonucleotide transferase-mediated dUTP nick-end labeling (TUNEL) staining, respectively, as previously described [57].

Histological analyses and immunostaining

Evaluations of histological and immunostaining of ventricular structure, Cx43 distribution and myocardium apoptosis were performed as previously described [30, 47].

Ca^{2+} transient imaging

NRVM Ca^{2+} transient measurement was performed by SP8 Leica confocal microscopy as previously described [30, 42, 57].

Immunoblotting

NRVM and heart tissue were lysed and their immunoblotting evaluations were performed as previously described [30, 57].

Antibodies

Antibodies used were as follows: rabbit anti-calnexin, anti-sodium potassium-ATPase, anti-Fas and anti-N-cadherin (Abcam), rabbit anti-Cx43-pS282 and anti-Cx43-pS279 (Biobyt), rabbit anti-p-p38 (Thr180/Tyr182), anti-p38 MAPKα, anti-Cx43-pS368, anti-Cx43-pS262, anti-Cx43 and anti-FADD (Santa Cruz), mouse anti-GAPDH and anti-β-actin (ZSGB-BIO), mouse anti-caspase-8 and anti-cytochrome C (Santa Cruz), mouse anti-Cox-IV and rabbit anti-protein phosphatase type 2A (PP2A-A) and anti-PP2A-B (CST), and goat anti-Cx43 (Acris). All antibodies were used at a ratio of 1:1000, except for anti-FADD antibody and anti-sodium potassium-ATPase antibody at a ratio of 1:500 and 1:10,000, respectively.

Statistical analysis

All experiments were performed at least four times to assess reproducibility of the results. Data are presented as mean ± SD, and were analyzed by Student's *t* test for unpaired observations. For multiple groups, two-way ANOVA was performed with post Tukey adjustment when appropriate. A p value of < 0.05 was considered statistically significant, and significant values were expressed as $^{*}p < 0.05$, $^{**}p < 0.01$, $^{***}p < 0.001$.

Results

Ischemia/reperfusion induced Cx43 dephosphorylation at S282 and cardiac injury in vivo

To explore whether Cx43 phospho-S282 is altered and thus causes *I*/*R*-triggered electrical disturbances and cardiomyocyte apoptosis by activating p38/Fas/FADD/caspase-8, a pathway found to be activated in S282-mutant-treated NRVMs and Cx43-S282A$^{+/-}$ mice [57], we first evaluated the Cx43-pS282 status in rats subjected to left coronary artery ligation following reperfusion (30 min/2 h) (Supplementary Fig. 1). ELISA analysis revealed that *I*/*R* rats displayed higher levels of lactate dehydrogenase (LDH) and cardiac troponin-I (cTn-I) in their blood sera than did the sham rats (Supplementary Fig. 2) as well as elevated S–T segments (18/22, 86.4%), premature ventricular beats (PVB; 8/22, 36.4%) and ventricular tachycardia (VT; 3/22, 13.6%) on the electrocardiogram (ECG) (Fig. 1a, b). In addition, we found caspase family activation, including caspase-8/-9/-3 detected by ELISA kits, myocardial infarct with enlarged extracellular space detected by 2,3,5-triphenyltetrazolium chloride (TTC) and hematoxylin and eosin (H&E) staining, respectively, and increased apoptotic cells detected by terminal deoxyribonucleotide transferase-mediated dUTP nick-end labeling (TUNEL) assays (Fig. 2a–c). Thus, these results demonstrated a typical heart injury, including myocardial apoptosis and infarction and arrhythmias upon *I*/*R* attack in a rat model.

Cx43 serine dephosphorylation is mainly regulated by serine/threonine protein phosphatase types 1 and 2A (PP1 and PP2A), particularly PP2A, which is increased in *I*/*R* hearts [1, 55]; hence, we evaluated the expressions of two PP2A subtypes using specific antibodies. A significant increase in PP2A-A, but not PP2A-B, expression was found in *I*/*R* ventricles compared with the sham hearts, consistent with previous findings [1, 14, 21]. In addition, p-p38 MAPKα (Thr180/Tyr182),

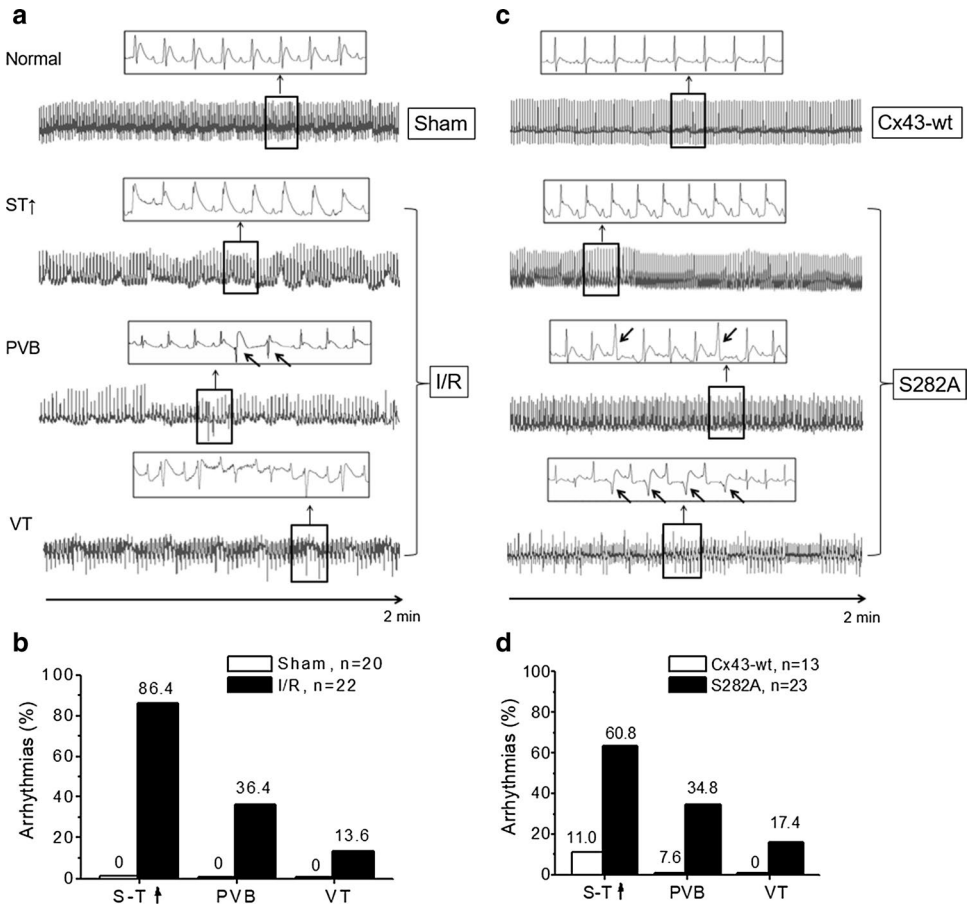

Fig. 1 Ischemia/reperfusion or S282A transfection into the left ventricle induced arrhythmias in rats. **a** Rats were subjected to ischemia/reperfusion (*I/R*, 30 min/2 h) treatment as described in "Materials and methods" and compared with sham rats. Representative ECG recordings 1 h after reperfusion showed S–T segment elevation, premature ventricular beats (PVB) and ventricular tachycardia (VT) in *I/R* rats, while all sham rats were normal. Oblique arrows indicate the premature beats. **b** Percentages of these abnormalities in *I/R* rats. **c** Representative ECG recordings display S–T elevation, PVB and VT in rats after *S282A*-gene transfection for 5 days in the left ventricular wall by intramyocardial injection. Oblique arrows indicate the ventricular arrhythmias. **d** Percentages of PVB and VT in S282A-transfected rats

the critical activation site of p38 in heart stress response [32, 34, 38], and Fas/FADD activations were increased in the *I/R* ventricles (Fig. 2d–f). Using specific antibodies for Cx43-serine sites via Western blot, we found increases in pS262 and pS368 levels, consistent with previous findings [51, 52], but a decrease in pS279 and pS282 abundance in *I/R* ventricles compared with sham ones. The Cx43 expression reduced slightly, while N-cadherin (N-Cad), the junctional protein in gap junction discs, remained unchanged (Fig. 2f, g). Here, expression of β-actin, but not GAPDH, was increased in *I/R* ventricle (Fig. 2f) and also in *A/R*-stimulated cells (Fig. 3f); hence, GAPDH was used as a reference protein in all Western blot experiments in this study. Ventricular staining with specific antibodies against Cx43 or pS282 revealed more Cx43 redistribution from the intercalated disc to the lateral edges of the myocytes, a process referred to as Cx43 lateralization [9, 10, 24, 31, 48], and reduced pS282 labeling in the *I/R* ventricles (Fig. 2h), supporting the Western blot detection (Fig. 2g).

Anoxia/reoxygenation induced Cx43 dephosphorylation at S282 and cardiomyocyte apoptosis in vitro

Next, we adopted monolayer NRVMs exposed to *A/R* (12/6 h) in vitro (Supplementary Fig. 1) to mimic *I/R* myocardial injury in vivo. Additionally, many studies, including this study, have demonstrated PP2A activation in *I/R*-injury hearts (Fig. 2), and inhibiting PP2A with a specific antagonist can effectively prevent heart injury from *I/R* [1, 14, 20, 23, 55]. Therefore, we evaluated the effect of 58 nM of cantharidinate (CA), a PP2A inhibitor, on *A/R*-induced cardiomyocyte damage. Functional evaluation showed changes in cell shape, coordinated spontaneous Ca^{2+} transients (indicative of normal electrical activity and gap coupling) and the potentiated Ca^{2+} signal response to phenylephrine (PE, an α-adrenoceptor agonist) in Fluo4-loaded NRVMs upon *A/R* (Fig. 3a, b). In addition, more apoptotic cells and higher

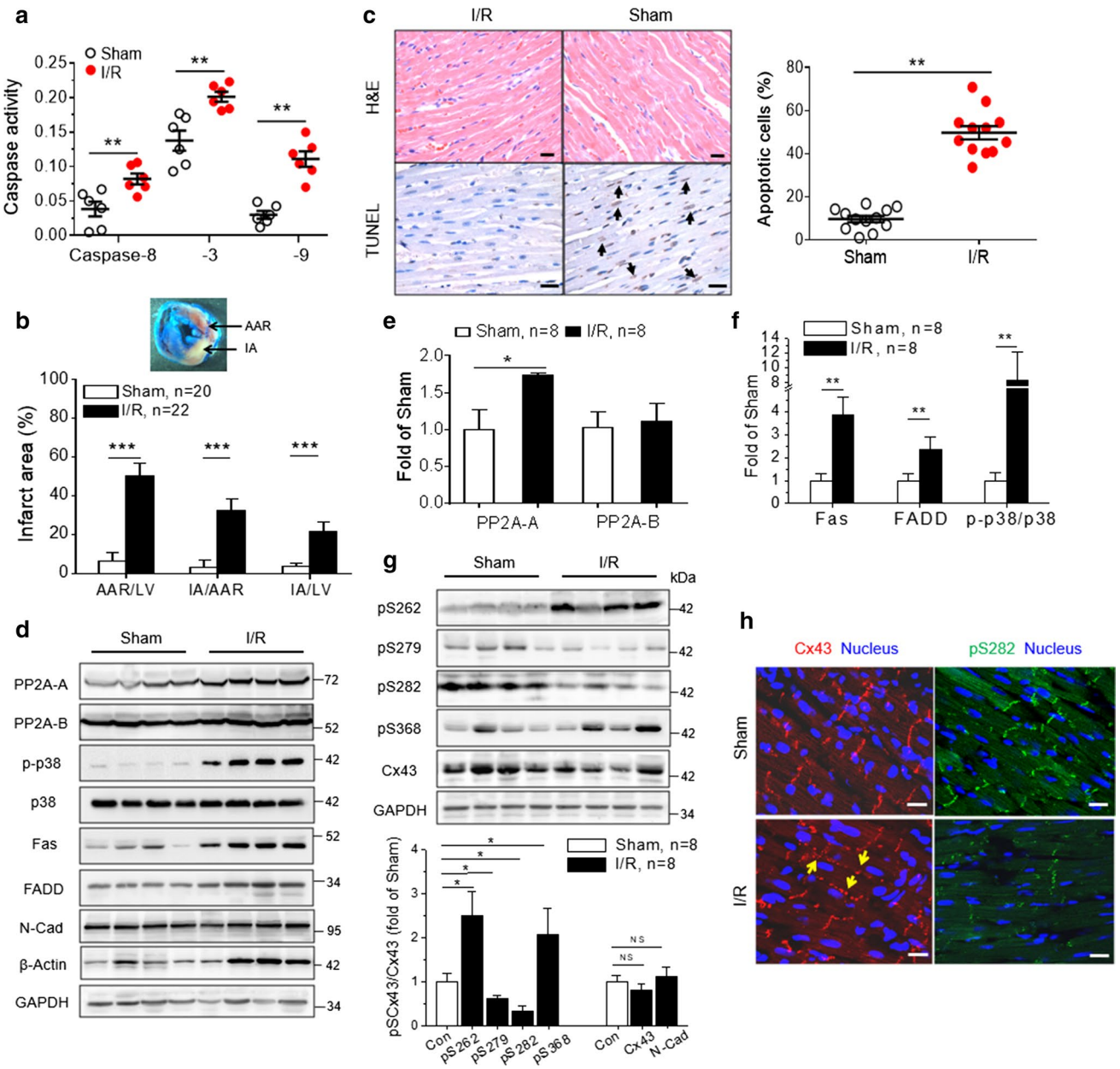

Fig. 2 Ischemia/reperfusion induced rat myocardial apoptosis and Cx43 phosphorylation changes. **a** Apoptosis in the *I/R* myocardium was determined by measuring caspase-8/-9/-3 activity using ELISA kits and compared with those in sham rats. **b** Left ventricle (LV) sections from sham and *I/R* rats were stained with Evans blue and 2,3,5-triphenyltetrazolium chloride, and the areas at risk (AAR), infarct area (IA) and LV were analyzed using ImageJ software. **c** Representative images of the LV from *I/R* and sham rats stained with H&E or terminal deoxyribonucleotide transferase-mediated dUTP nick-end labeling (TUNEL), and TUNEL-positive cells indicated with arrows were increased in *I/R* ventricles compared with sham rats. **d** Abundances of PP2A, PP2B, p-p38, p38, Fas, FADD and N-Cad were determined by Western blot using specific antibodies. **e** PP2A and PP2B fold changes in *I/R* ventricles relative to those in sham rats (after normalization with GAPDH) were detected. **f** Fas, FADD and p-p38 fold changes after normalization with GAPDH or p38 in *I/R* ventricles relative to those in sham rats were detected. **g** Cx43 phosphorylation at S262, S368, S279 and S282 was determined by specific antibodies and fold changes in pS262, pS368 and pS282 after normalization with Cx43, and total Cx43 and N-Cad expressions (after normalization with GAPDH) relative to those in sham rats. **h** Cx43 lateralization (indicated with arrows) and a weak signal in pS282 labeling were observed in *I/R* ventricles stained with antibodies specific for pS282 or Cx43 and compared with sham ventricles. Nuclei were stained with Hoechst 33342. Scale bar 30 μm, the number of animals is indicated in each panel, except for 5 rats in **h**. Data are the mean ± SD, $*p < 0.05$, $**p < 0.01$, $***p < 0.001$, NS, no significant difference, unpaired two-tailed Student's *t* test

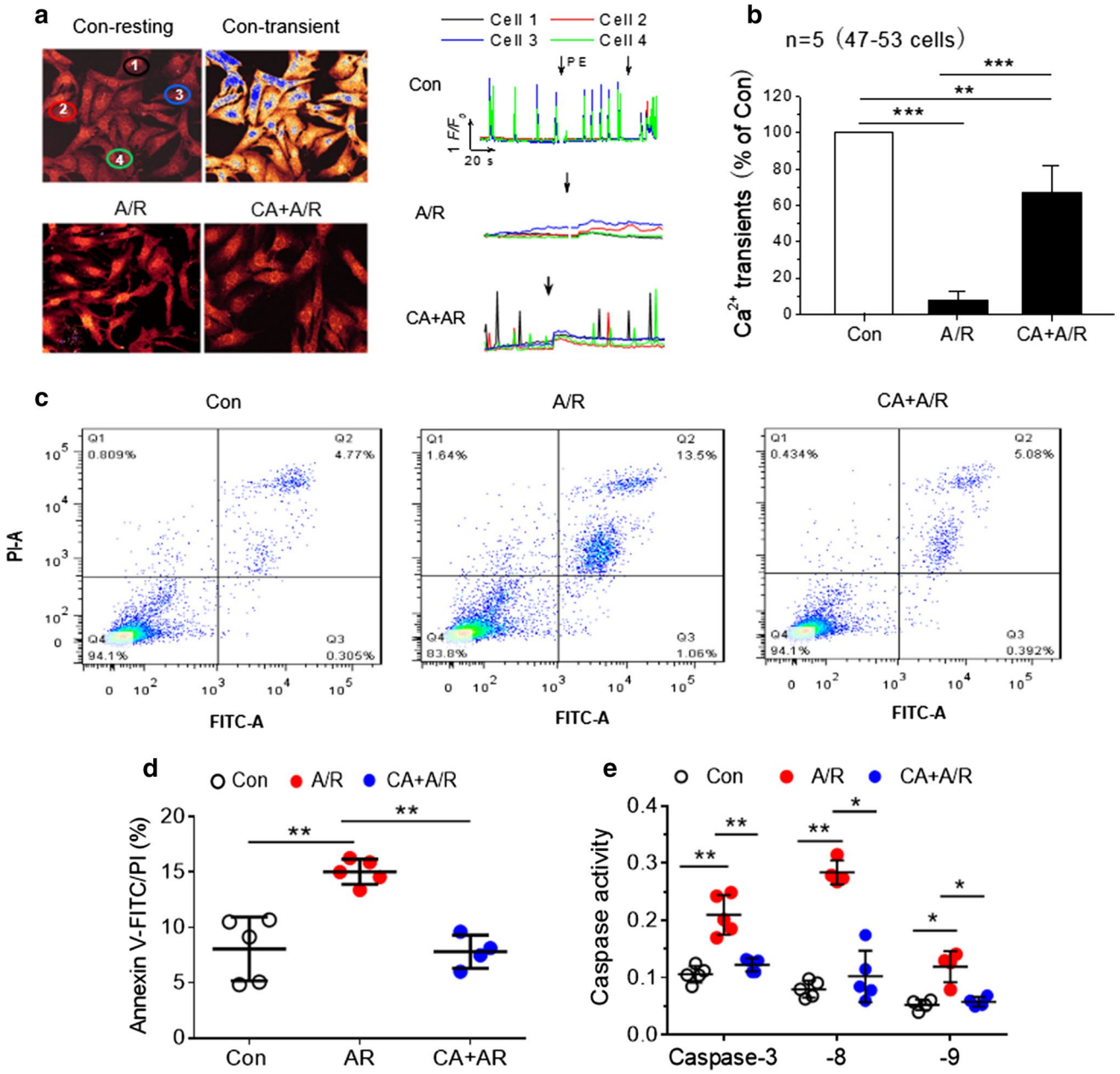

Fig. 3 Anoxia/reoxygenation induced cantharidinate-sensitive Ca^{2+} signaling abnormalities and cell apoptosis. **a** Representative images and traces of Fluo-4-loaded monolayer NRVMs under condition of normoxia or anoxia/reoxygenation (*A/R*, 12/6 h) show a change in cell shape, and suppressions of spontaneous Ca^{2+} transients and the phenylephrine (PE, 10 μM) induced potentiation effect on Ca^{2+} transients in *A/R* cells. **b** Quantitative analyses of the spontaneous Ca^{2+} transients in these groups. Pretreatment of cells with cantharidinate (CA, 58 nM) for 10 min and present until harvest partially recovered these abnormal changes due to *A/R*. **c** Apoptosis in NRVMs exposed to *A/R* with or without CA was determined by Annexin V-FITC/PI staining using flow cytometry. **d** CA inhibited NRVM apoptosis due to *A/R*. **e** NRVM apoptosis due to *A/R* was also determined by measuring the activities of caspase-3/-8/-9 using ELISA kits, and CA inhibited the *A/R*-induced caspase activation. Data are the mean ± SD, $*p < 0.05$, $**p < 0.01$, $***p < 0.001$, two-way analysis of variance (ANOVA)

caspase-8/-9/-3 activity were found in *A/R* cells than in normoxic cells (Fig. 3c–e). Pretreating cells with CA recovered ~ 60% of the spontaneous Ca^{2+} transients and inhibited apoptotic damage in the *A/R* cells. Accordingly, PP2A-A and p38, but not PP2A-B, were activated, and enhanced physical interactions between Cx43/p38 and Cx43/PP2A-A were observed in the *A/R* cells (Fig. 4a–c). Fas/FADD were also activated but completely inhibited by CA in the *A/R* cells (Fig. 4d). Further, specific antibodies were used to assess Cx43 phosphorylation via Western blot. Increased phosphorylation at S262 and S368, but dephosphorylation at S279 and S282, relative to the total Cx43 was found in *A/R*

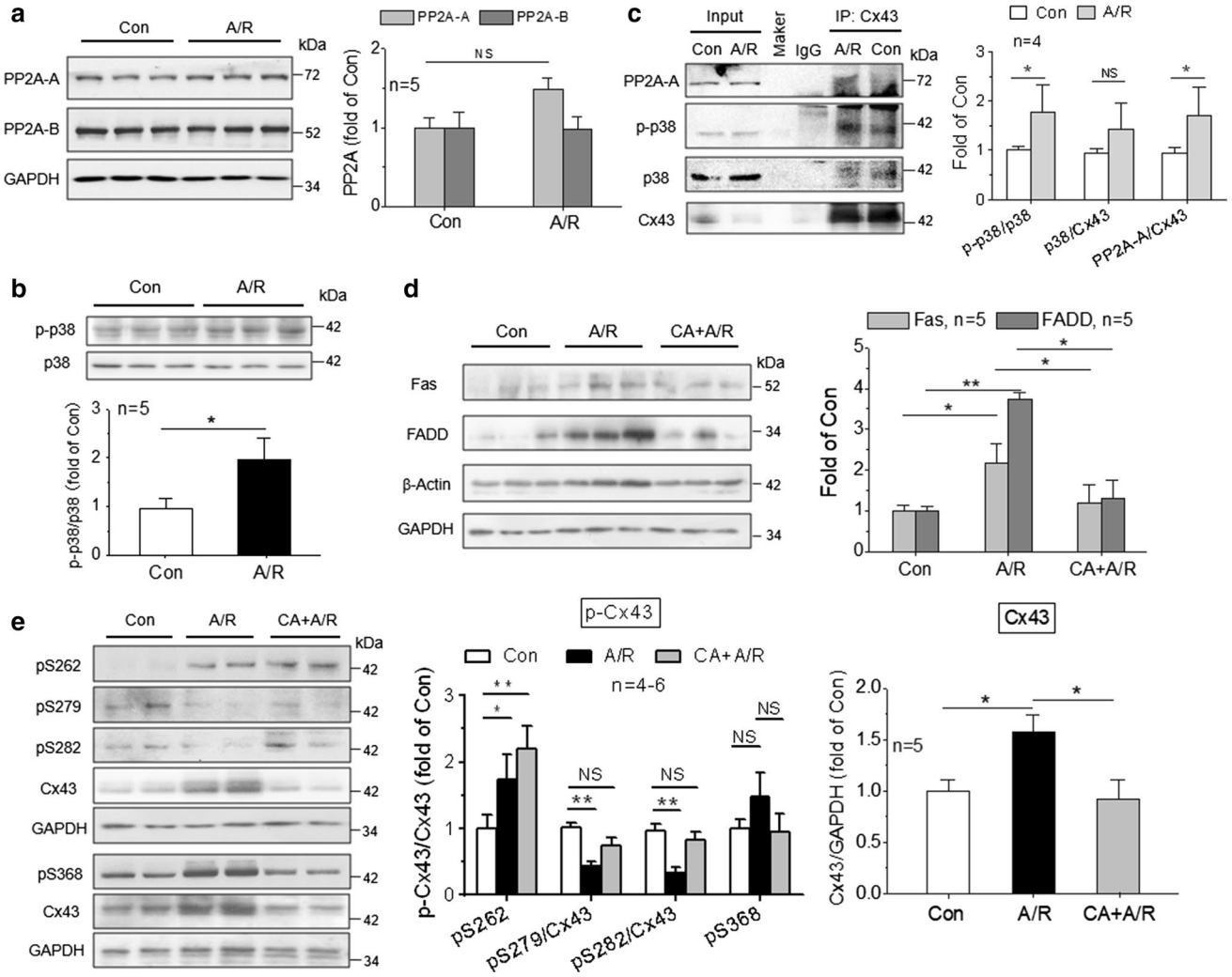

Fig. 4 Anoxia/reoxygenation induced p38 and PP2A activations and Cx43 dephosphorylation at S282. **a** Lysates from NRVMs under conditions of normoxia or *A*/*R* were analyzed by Western blot, and fold increases in PP2A-A and PP2A-B relative to those of normoxic cells (Con) (after normalization with GAPDH) were detected. **b** Fold increase in p-p38/p38 was detected by Western blot in *A*/*R* cells. **c** Lysates from NRVMs under condition of normoxia or *A*/*R* were immunoprecipitated with anti-Cx43 antibody and then Western blotted with anti-p-p38, anti-p38 or anti-PP2A antibody, and fold changes in p-p38/p38, p38/Cx43 and PP2A/Cx43 in *A*/*R* cells relative to those of the control were detected. $N=4$ independent experiments for each treatment. **d** Lysates from control or *A*/*R*-treated NRVMs with DMSO or CA (58 nM) pretreatment for 10 min were analyzed by Western blot, and fold changes in Fas and FADD relative to those of the control were detected (after normalization with GAPDH). **e** Cx43-pS262, pS368, pS279 and pS282 and total Cx43 expressions relative to those of the control were detected (after normalization with GAPDH). $N=4$–5 dishes of cultured NRVMs from at least 80 rat hearts as indicated in each panel. Data are the mean ± SD, $^*p<0.05$, $^{**}p<0.01$, NS, no significant difference, unpaired two-tailed Student's *t* test (**b**, **c**) and two-way ANOVA (**d**, **e**)

cells compared with normoxic cells. As expected, inhibiting PP2A with CA abolished S279 and S282 dephosphorylation, and unexpectedly, increased pS262, but not pS368, under anoxic conditions (Fig. 4e). This suggests that PP2A may have directly or indirectly mediated the altered phosphorylation at S279, S282 and S368, but not the altered S262, during *I*/*R*. pS368 upregulation in ischemic hearts has been found to result from S365 dephosphorylation [51]; hence, PP2A likely regulates S365 dephosphorylation, which subsequently reduces pS368 increase.

Cx43 also expresses in mitochondria and is involved in the regulation of mitochondrial function [5, 33]. Importantly, cardiac mitochondrial Cx43 contributes to ischemic preconditioning-induced myocardium protection effect [6, 7, 20, 41]. Here, in this study, the mitochondrial apoptotic pathway is also activated in *A*/*R* cells as previously reported [4, 8, 15, 20] because caspase-9 was activated (Fig. 3e) and cytochrome C (Cyt-C) was released from the mitochondria to the cytoplasm (Supplementary Fig. 3). The level of pS282 in the mitochondria was not significantly altered upon

A/*R* stimulation (Supplementary Fig. 3) and in heterozygous Cx43-S282A mice [57]. This may indicate that Cx43 dephosphorylation upon S282-related cardiomyocyte injury is not closely associated with the mitochondrial pathway; thus, we did not further investigate the Cx43-pS282 involved in the mitochondrial pathway.

S282A intramyocardial injection induced cardiac dysfunction, arrhythmias and myocardial apoptosis

These data above demonstrated an obvious Cx43 dephosphorylation at S279/282 accompanied by arrhythmias and myocardial apoptosis under ischemic conditions. In addition, previous studies found a proapoptotic effect of the S282A mutant on cultured NRVMs and serine 282 phosphorylation also regulates the phosphorylation of S279 [25, 53, 57]. Thus, we performed an in vivo study in three groups of rats receiving intramyocardial injections of a vector or virus carrying either the *S282A* or *Cx43-wt* genes under ultrasound guidance to investigate a possible causal role of S282 dephosphorylation in heart injury [42]. Four sites in the left ventricular anterior wall were selected and injected with 100 µl saline or an equal volume of saline containing the virus (Fig. 5a). All animals had normal ECG measurements before and until the 2nd day post-viral transfection. On day 3 post-injection, three of twenty-three S282A-transfected rats developed accidental premature ventricular tachycardia (data not shown), and more than half of these rats had persistent arrhythmias 2 days later; therefore, all data were collected on day 5 post-transfection (Supplementary Fig. 1). Positive green fluorescent protein (GFP) and HA-antibody staining indicated a successful viral transfection into the left ventricular myocardium (Fig. 5a, b). Disarranged myocardium (indicated with long yellow arrow) with Cx43 lateralization (short yellow arrows) and pS282 disappearance in the damaged myocardium but appearing intermittently at the end of myocytes (white arrows) was found in S282A rats (Fig. 5b). In addition, functional changes, including significant decreases in the ejection fraction (EF), fractional shortening (FS) and left ventricular anterior wall thickness at systole (LVAW;s), were observed, whereas left ventricular posterior wall thickness at systole (LVPW;s) where the *S282A* gene was absent remained unaltered (Fig. 5c and Supplementary Table 1). Similar to the *I*/*R* rats, S282A rats also displayed S–T elevation (14/23, 60.8%), PVB (8/23, 34.8%) and VT (4/23, 17.4%) (Fig. 1c, d). Moreover, obvious local myocardial defects were found in three of five tested rats receiving S282A mutants (indicated with an arrow), and distorted myocardial fibers and many TUNEL-positive myocytes appeared in the para-defect areas (Fig. 6a). Increased Fas/FADD expression and caspase-8/-3 activity and p38 activation also occurred in the S282A ventricles (Fig. 6b–e). Western blot analysis of the injected area showed considerably reduced pS282 expression after normalization with Cx43 in the S282A ventricles compared with that in the vector-treated ventricles (Supplementary Fig. 4). Thus, these results demonstrated an *I*/*R*-like cardiac injury including arrhythmias and myocardial apoptosis due to direct ventricular transfection of the *S282A* gene.

Cx43 S282A heterozygous mice displayed animal death, arrhythmias, cardiac dysfunction and dispersed myocardial apoptosis

In a previous study, significant changes, including arrhythmias, myocardial apoptosis and fibrosis, were found in heterozygous Cx43-S282A mice, while homozygous mice failed to be generated. Notably, heterozygous mice exhibited different degrees of ventricular arrhythmias; that is, some mice without significant changes in pS282 retained generally normal cardiac electrical activity and cell homeostasis (referred to as Het1), whereas others with moderate or severely decreased pS282 had moderate to severe ventricular arrhythmias and myocardial apoptosis/fibrosis (referred to as Het2 and Het3). Such S282 dephosphorylation-dependent pathological alterations occurring under basal conditions suggest that intrinsic pS282 plays an essential role in regulating cardiomyocyte survival and electrical stability in vivo [57].

In this study, we further evaluated the relationship between survival rate, cardiac function and dispersed myocardial injury and pS282 levels among the three groups of heterozygous mice measured on days 12–21 after birth (Supplementary Fig. 1). All Het3 mice died within 20 days after birth, while mice above 95% Het2 and 100% Het1 developed to maturation (Fig. 7a). Interestingly, similar to S282A-transfected rats, both Het2 and Het3 mice had more and severer spontaneous ventricular arrhythmias and S–T change (Fig. 7b, c. S–T change was not detectable in Het3 mice because of persistent VT) than did the S282A rats (Fig. 1c, d) and significantly decreased EF and FS compared with those in WT mice (Fig. 7e and Supplementary Table 2). These pathological changes including death rate, lowered EF and ventricular arrhythmias (PVB and VT were arbitrarily measured as 20% and 40% in severity) and myocardial apoptosis [57] were tightly correlated with cardiac Cx43-pS282 levels (Fig. 7f). Moreover, while local myocardial injury and decreased LVAW;s were found in the S282A injected area (Figs. 5, 6), both the right and left ventricles in the Het2 mouse displayed dispersed widen extracellular space, cardiomyocyte apoptosis (Fig. 8a, b) and decreased LVAW;s and LVPW;s (Fig. 7e), further supporting the hypothesis that myocardial injury depends on deficient Cx43 phosphorylation at S282.

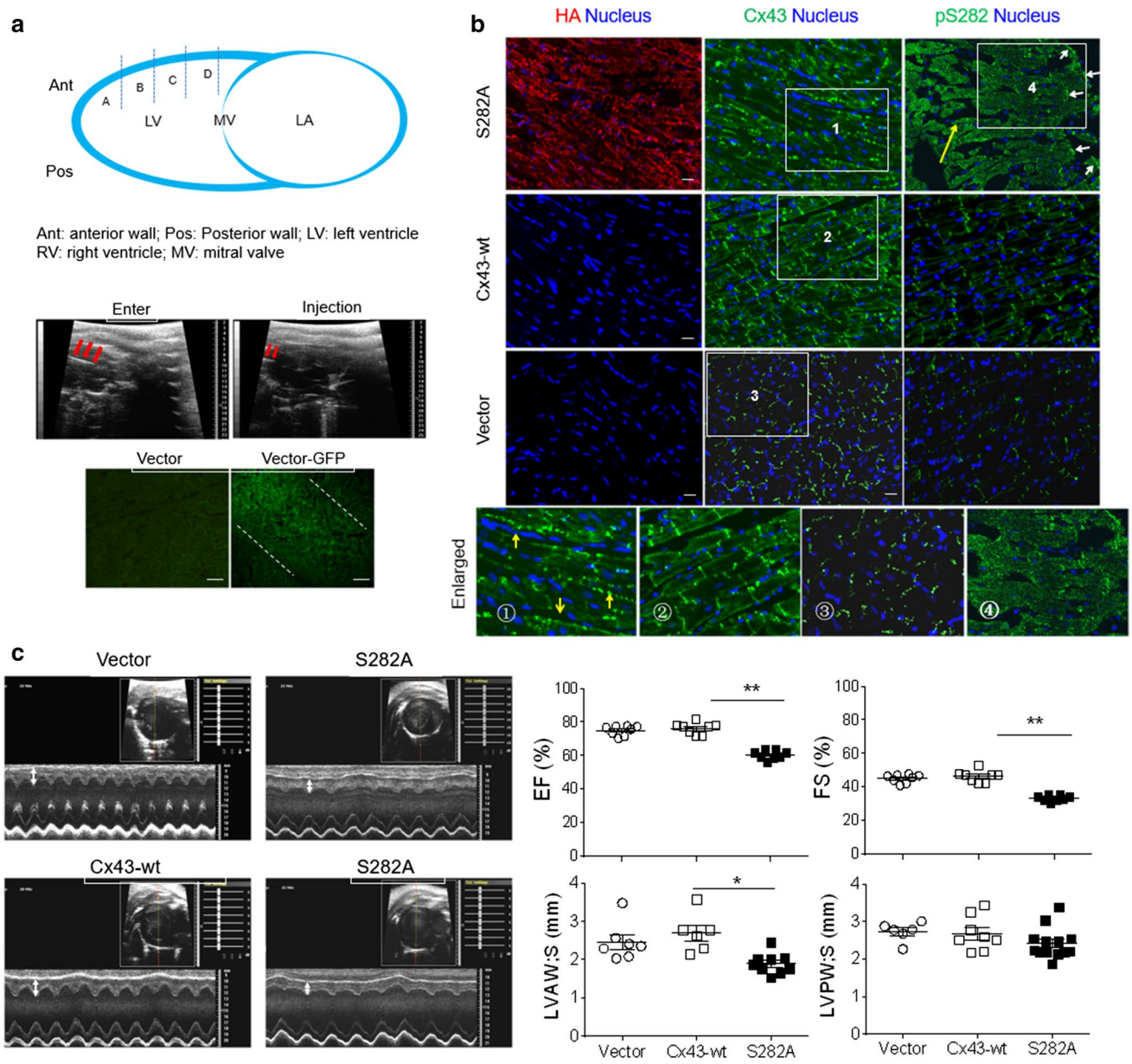

Fig. 5 S282A expression induced myocardial injury and Cx43 lateralization in rats. **a** Plot of four injection sites in left ventricular anterior walls of rats (A–D) and an overview of the ultrasound-facilitated myocardial transfection of the *S282A* or *Cx43-wt* genes. Arrows indicate the needle for entering and injecting. Enhanced GFP labeling in vector-GFP-transfected ventricles at day 3 indicated successful viral infection. Scale bar 100 µm. **b** Representative images of gene-transfected ventricles for 5 days stained with antibodies specific for HA, Cx43 and pS282, respectively. White arrows and long and short yellow arrows indicate the remaining pS282, disarranged myocardium and obvious Cx43 lateralization in the S282A-transfected area, respectively. The square frames with number 1–4 in it indicate the panels below of enlarged interested areas. Nuclei were stained with Hoechst 33342. Scale bar 30 µm. **c** Rat echocardiographic images and data analysis on day 5 after transfection. Double arrows indicate decreased left ventricular anterior wall thickness at systole (LVAW;s); but no change in posterior wall thickness at systole (LVPW;s) in S282A rats. Assessments of ejection fraction (FS), fractional shortening (EF) (upper panels in left) and LVAW;s and LVPW;s (lower panels in left) were detected and compared with those of Cx43-wt rats. $N = 5$ rats for **a**, **b** and 8 for **c** in each group as indicated. Data are the mean ± SD, $^{**}p < 0.01$, unpaired two-tailed Student's *t* test

Discussion

Arrhythmias and myocardial infarction are common events in myocardial ischemia and the leading cause of mobility and mortality among heart diseases. Alterations in Cx43 function or topology, the critical cardiac gap junction protein, contribute profoundly to electrical disturbances and myocardial injury in *I/R* hearts. As in many cardiac pathologies, Cx43 remodeling, including Cx43 dephosphorylation, decreased Cx43 expression at the intercalated

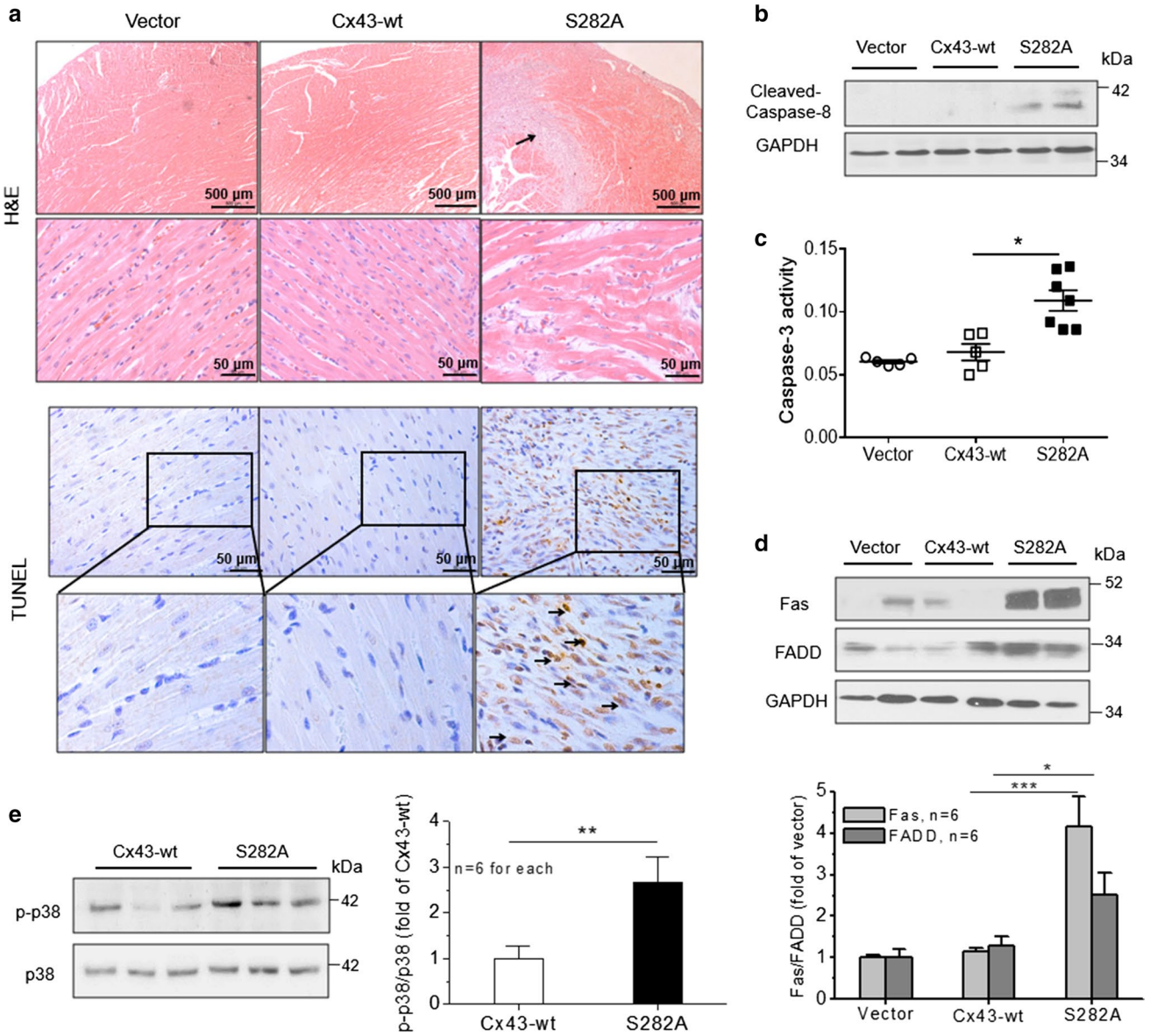

Fig. 6 S282A expression induced rat local myocardial apoptosis. **a** Representative images of S282A-mutant-transfected ventricles stained with H&E or TUNEL as indicated. Arrows indicate a myocardial defect area in the H&E image and TUNEL-positive cells in the TUNEL image. Scale bars are as indicated. **b** Lysates from the locally injected ventricle were analyzed by Western blot, and caspase-8 activation was detected. **c** Activity of caspase-3 was determined by ELISA. **d** Fas/FADD expressions and fold increases relative to those of the vector ventricles (after normalization with GAPDH) were detected. **e** Fold increase in p-p38 after normalization with p38 was detected. $N=5$ mice for **a** in each group and other panel numbers as indicated. Data are the mean ± SD, $*p<0.05$, $**p<0.01$, $***p<0.001$, unpaired two-tailed Student's *t* test

disc and Cx43 lateralization in the ventricle, is the key trigger of arrhythmias and vulnerability of cardiomyocyte apoptosis in myocardial ischemia and nonischemic stresses [9, 10, 24, 29, 31, 44, 46, 48, 50]. However, although the causal role of Cx43 as an arrhythmogenic substrate is established, the exact site(s) that directly trigger arrhythmias and the mechanism(s) underpinning the pathological action of Cx43 in cell death are poorly understood.

We previously found that Cx43 dephosphorylation at S282 caused both arrhythmias and cardiomyocyte apoptosis under normal conditions, demonstrating this site's important role in cardiomyocyte homeostasis [57]. In this study, we asked whether cardiac *I*/*R* conditions induce Cx43-S282 dephosphorylation, which is involved inducing the arrhythmias and myocardial apoptosis due to *I*/*R* attack. We found significant Cx43 dephosphorylation at S282 in both *I*/*R*

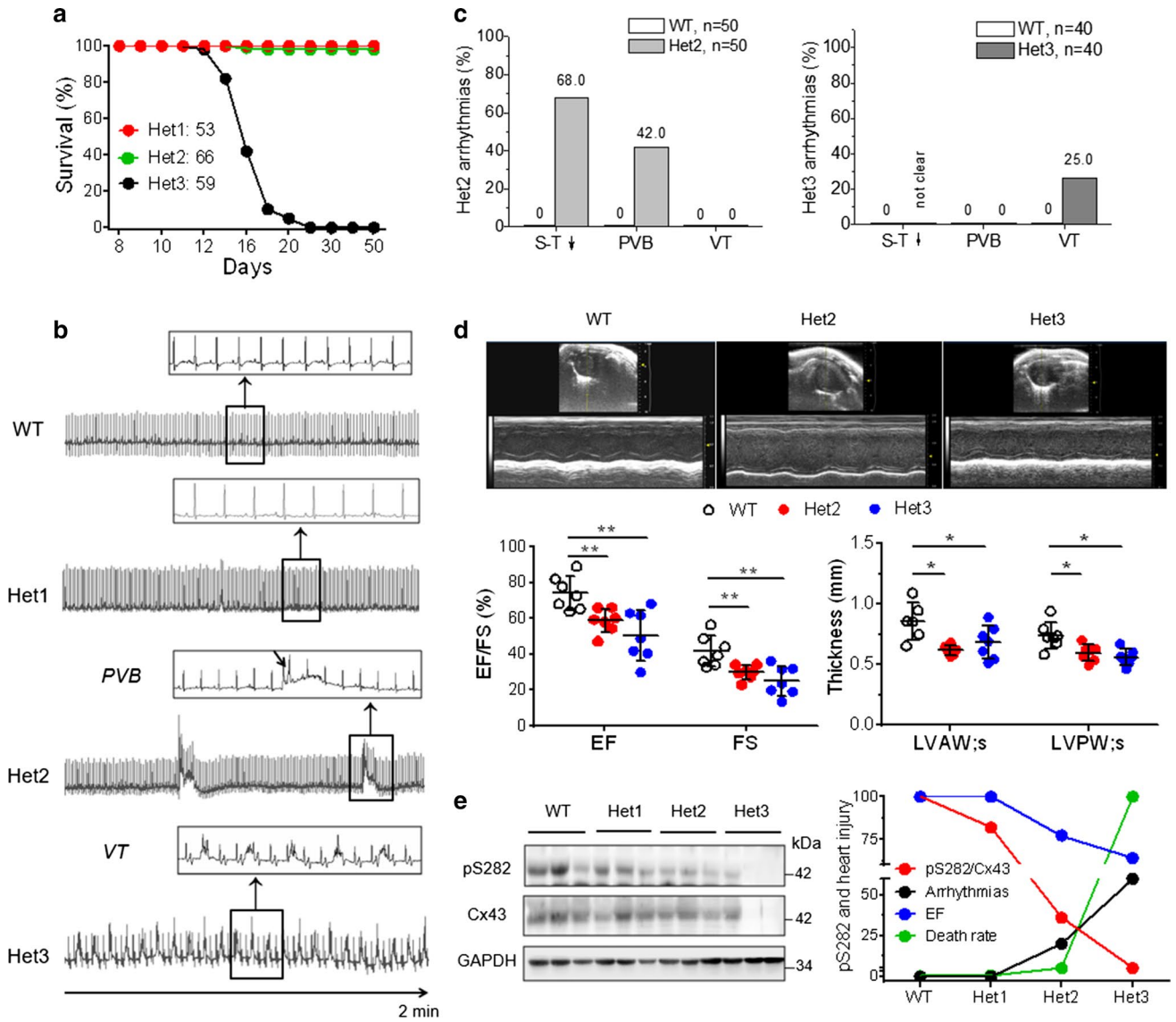

Fig. 7 Cx43-S282A$^{+/-}$ mice exhibited dispersed myocardial damage and apoptosis. **a** Neonatal lethality occurred between days 9 and 21 after birth in all Het3 mice, while 98% and no deaths were found in Het2 and wild-type mice (WT) mice. **b** Representative ECG recordings showed S–T segment reduction, PVB and VT in Cx43-S282A heterozygous mice on day 12 after birth. An oblique arrow indicates abnormal beat. **c** Percentages of S–T elevation, PVB and VT were analyzed. **d** Mouse echocardiographic images and data analysis of EF, FS, LVAW;s and LVPW;s in S282A-heterozygous mice compared with those in WT mice. **e** Lysates from ventricles of WT and Het1–3 were analyzed by Western blot, and pS282 and Cx43 were detected with specific antibodies. Cardiac damage, including arrhythmias, animal death and cardiac dysfunction were well correlated with the abundance of S282 dephosphorylation in heterozygous mouse ventricles. Data are the mean ± SD, $*p < 0.05$, $**p < 0.01$, unpaired two-tailed Student's *t* test

hearts and NRVMs exposed to *A*/*R* (Figs. 2g, 4e), accompanied by S–T elevation and ventricular tachycardia in *I*/*R* rats and depressed or uncoupled Ca^{2+} transients in *A*/*R*-treated NRVMs (Figs. 1a, b, 3a, b). Apparent ischemic cardiomyocyte death with p38/Fas/FADD/caspase-8/caspase-3 pathway activation was also observed in both the *I*/*R* ventricles and *A*/*R*-treated NRVMs (Figs. 2, 3 and 4 and Supplementary Fig. 2). Importantly, the S282A viral infection in the anterior wall of the left ventricle mimicked the *I*/*R* injuries in manifestations of ventricular tachycardia (Fig. 1c, d), local myocardial defect (infarction)/apoptosis and p38/Fas/FADD/caspase-8 pathway activation (Figs. 5, 6). In addition, S282A ventricles displayed Cx43 lateralization (Fig. 5b, enlarged panels ① and ②) and pS282 disappearance (Fig. 5b, enlarged panel ④) in the injured area similar to the Cx43 changes displayed in the *I*/*R* ventricles (Fig. 2h). Heterozygous Cx43-S282A mice further confirmed the relationship between the deficient S282 phosphorylation and heart injury, in which

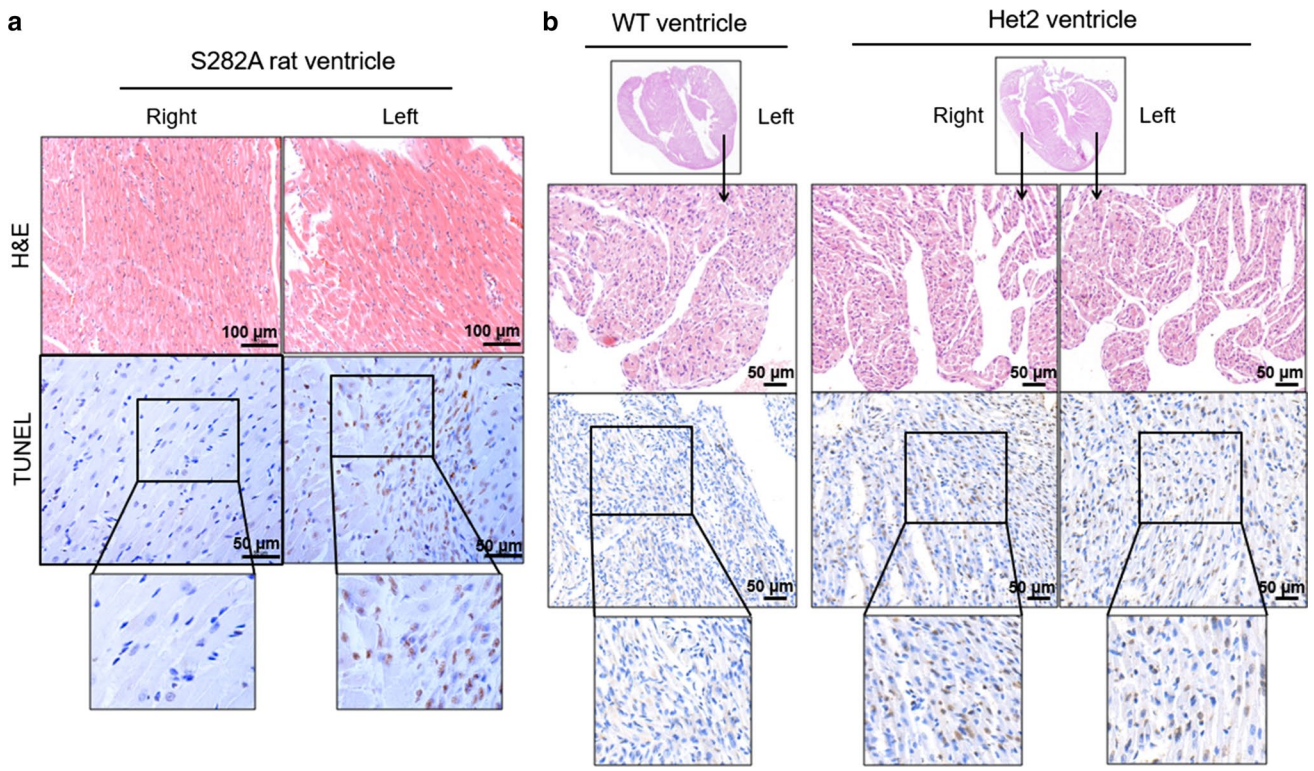

Fig. 8 Comparison of myocardial injury between Cx43-S282A$^{+/-}$ mice and heart S282A transfected rats. **a** Rat with left ventricle anterior wall intramyocardial transfection of *S282A* gene stained with H&E and TUNEL shows spotted damage and cardiomyocyte apoptosis. **b** Left and right ventricles from Cx43-S282A$^{+/-}$ mice 2 (Het2) display increased extracellular space and dispersed myocardium apoptosis in whole field, while wild-type ventricles do not have noticeable changes. Scale bar as indicated, $n=6$ animals for each group in each panel

the death rate, ventricular tachycardia, cardiac dysfunction, global myocardial apoptosis and lowered thickness in the ventricular wall in the mice were all tightly correlated with the pS282 level, compatible with the changes that occurred in the rats' left ventricular anterior walls where S282A-mutant transfection induced local S282 dephosphorylation (Figs. 6, 7 and 8). Therefore, both the in vivo S282 dephosphorylation-manipulating models and the in vitro cell model support the hypothesis that S282 dephosphorylation alone is sufficient to trigger and sustain the electrical disturbance and cardiomyocyte apoptosis in *I/R* hearts.

As a crucial channel for rapid electrical signal propagation and cardiac muscle contraction synchronization, changes in Cx43 function or topology are considered a key proarrhythmic substrate. Cx43 dephosphorylation upon ischemic injury has been shown to occur very early and can prevent propagation of apoptotic signals from the damaged region through Cx43 gap junction channels to the adjacent myocardial cells [18, 28, 32, 51, 54, 56]. In turn, however, it also causes slow or even blocked electrical diffusion among cardiomyocytes and promotes inducible arrhythmias [19, 29, 35, 44, 54]. Multiple studies have found that changes in individual phosphorylated residues within the Cx43-CT domain are linked with inducing ischemic arrhythmias. For example, animals with S297, S356, S255, S368 or S325/328/330 dephosphorylation, respectively, all exhibit high propensities to arrhythmias upon ischemic stimulation, while mimicking their phosphorylation shows resistance to proarrhythmic stimulations [12, 29, 37, 39, 45, 50, 51]. To our knowledge our findings are the first to suggest that dephosphorylation of one Cx43 phosphosite, S282, not only induces arrhythmia vulnerability when stimulated by injury (data not shown) but is sufficient to trigger ventricular tachycardia under resting conditions. The heterozygous mice with obvious deficient S282 phosphorylation have arrhythmias detected after birth. Hence, these observations indicate an important role of S282 phosphorylation in maintaining electrical stability in cardiomyocytes and interestingly revealed a common characteristic: the high occurrence of elevated S–T segments in *I/R* rats and S282A-transfected rats (Fig. 1) but lowered S–T segment in S282A$^{+/-}$ mice (Fig. 7b, c), the lowered S–T segment is likely due to the long period of injury in S282A$^{+/-}$ mice. This may suggest that deficient Cx43-S282 phosphorylation affects the repolarization process of action potentials in cardiomyocytes;

however, the underlying mechanism and its significance for ischemic hearts require further investigation.

Myocardial apoptosis and necrosis resulting from *I/R* are fundamental causes of cardiac infarction and dysfunction. High-grade apoptosis occurs predominantly during reperfusion and plays an important role in determining infarct size, extent of left ventricular remodeling and development of early symptomatic heart failure after cardiac ischemia. Multiple proapoptotic substrates, such as reactive oxygen species generation, autoimmune response and excess ATP consumption, are implicated to be associated with activating the intrinsic (mitochondrial) or extrinsic (death receptor) apoptotic pathways and inducing cardiomyocyte death [8, 10, 15, 43]. In addition, accumulating evidence has documented that Cx43 plays an important role in regulating cell survival and death processes and participating in severe cardiac lesions through mostly undefined mechanisms [8, 10, 31, 47, 48]. Specific serine sites including S368, S262, S365 and S325/328/330 are reported to be dephosphorylated during cardiac ischemia or *I/R*. Mimicking null-phosphorylation at these sites sensitizes the heart to ischemic death and electrical instability upon ischemic stimuli [3, 27, 39, 49, 51, 52], while promoting Cx43 phosphorylation at S262 or S368 via fibroblast growth factor, sphingosine-1-phosphate, diazoxide or phosphatase inhibitors protects against *I/R*-induced myocardial damage [13, 24, 36, 52]. As with triggering myocardium apoptosis, to our knowledge, our findings are the first to suggest that deficient Cx43-S282 phosphorylation constitutively induces cardiomyocyte death. This harmful effect occurs specifically in the myocardium independently of deficient Cx43 expression or change in other residual dephosphorylation [57]. Importantly, regional S282 dephosphorylation by S282A transfection into the left ventricle exhibited similar myocardial injury as in the *I/R* ventricles, including S282 dephosphorylation, local cardiomyocyte apoptosis/infarction and Cx43 lateralization. Cx43-S282A$^{+/-}$ mice also demonstrated identical pathological changes in whole hearts, exhibiting S282 dephosphorylation-associated animal death, arrhythmias, and myocardial dysfunction and apoptosis, suggesting that S282 dephosphorylation may be involved in *I/R*-induced myocardial injury.

Enhanced PP2A activity in several heart diseases, including *I/R* ventricles, has been linked to Cx43 dephosphorylation and myocardial lesions through their physical interactions [1, 14, 21, 23, 56]. Preventing Cx43 dephosphorylation by phosphatase inhibitors has been explored and is considered beneficial in reducing myocardial damage and disordered electrical activity during *I/R* [14, 21, 23, 24, 56]. Interestingly, in addition to interacting with PP2A [1, 56], Cx43 also physically interacts with and can activate p38 (Fig. 4c) [32, 40, 57], thus activating the Fas/FADD/caspase-8 pathway and cardiomyocyte death [32, 38, 57]. Both p38 and Fas are critical signal proteins involved in *I/R*-induced myocardial cell death in animal models and ischemic patients [11, 16, 22, 32, 38, 40]. Herein, high abundances of PP2A-A, p-p38 and Fas/FADD with enhanced interactions between Cx43/PP2A-A and Cx43/p38 were observed in AR-treated NRVMs (Fig. 4c), and importantly, these observations are consistent with the findings in the Cx43-S282A$^{+/-}$ mouse ventricles [57]. Inhibiting PP2A with cantharidinate prevented cardiomyocyte apoptosis due to *A/R*, which is consistent with the effect observed in the *I/R* hearts [14, 19, 21, 23, 56]. These findings demonstrate that enhanced PP2A activity mediate serine S282 dephosphorylation, which acts as a linking point to the apoptotic pathway activation during *I/R*.

In summary, our results demonstrated for the first time, a robust Cx43 dephosphorylation at S282 in cardiomyocytes in vivo and in vitro upon *I/R* injury. Importantly, deficient S282 phosphorylation is linked to ventricular arrhythmias and cardiomyocyte apoptosis in *I/R* hearts. Based on observations from this study, we anticipate that recovery of S282 phosphorylation improves electrical stability, reduces arrhythmias, and limits apoptotic responses to ischemic attacks. Therefore, this intervention should be of great importance in treating cardiac ischemic damage as well as a potential candidate target for protecting the heart against myocardial injury and electrical disturbances during *I/R*.

Acknowledgements This work was supported by the National Natural Science Foundation of China (81370339, 81570206) and the Scientific Research Key Program of Beijing Municipal Commission of Education (KZ201710025023).

Compliance with ethical standards

Conflict of interest The authors declare that they have no conflicts of interest.

References

1. Ai X, Pogwizd SM (2005) Connexin 43 downregulation and dephosphorylation in nonischemic heart failure is associated with enhanced colocalized protein phosphatase type 2A. Circ Res 96:54–63. https://doi.org/10.1161/01.RES.0000152325.07495.5a
2. Akhmedov A, Montecucco F, Braunersreuther V, Camici GG, Jakob P, Reiner MF, Glanzmann M, Burger F, Paneni F, Galan K, Pelli G, Vuilleumier N, Belin A, Vallée JP, Mach F, Lüscher TF (2015) Genetic deletion of the adaptor protein p66Shc increases susceptibility to short-term ischaemic myocardial injury via intracellular salvage pathways. Eur Heart J 36:516–526. https://doi.org/10.1093/eurheartj/ehu400
3. Axelsen LN, Stahlhut M, Mohammed S, Larsen BD, Nielsen MS, Holstein-Rathlou NH, Andersen S, Jensen ON, Hennan JK, Kjølbye AL (2006) Identification of ischemia-regulated phosphorylation sites in connexin43: a possible target for the antiarrhythmic peptide analogue rotigaptide (ZP123). J Mol Cell Cardiol 40:790–798. https://doi.org/10.1016/j.yjmcc.2006.03.005

4. Bodendiek SB, Raman G (2010) Connexin modulators and their potential targets under the magnifying glass. Curr Med Chem 17:4191–4230
5. Boengler K, Ruiz-Meana M, Gent S, Ungefug E, Soetkamp D, Miro-Casas E, Cabestrero A, Fernandez-Sanz C, Semenzato M, Di Lisa F, Rohrbach S, Garcia-Dorado D, Heusch G, Schulz R (2012) Mitochondrial connexin 43 impacts on respiratory complex I activity and mitochondrial oxygen consumption. J Cell Mol Med 16:1649–1655. https://doi.org/10.1111/j.1582-4934.2011.01516.x
6. Boengler K, Konietzka I, Buechert A, Heinen Y, Garcia-Dorado D, Heusch G, Schulz R (2007) Loss of ischemic preconditioning's cardioprotection in aged mouse hearts is associated with reduced gap junctional and mitochondrial levels of connexin 43. Am J Physiol Heart Circ Physiol 292:H1764–H1769
7. Boengler K, Dodoni G, Rodriguez-Sinovas A, Cabestrero A, Ruiz-Meana M, Gres P, Konietzka I, Lopez-Iglesias C, Garcia-Dorado D, Di-Lisa F, Heusch G, Schulz R (2005) Connexin 43 in cardiomyocyte mitochondria and its increase by ischemic preconditioning. Cardiovasc Res 67:234–244. https://doi.org/10.1016/j.cardiores.2005.04.014
8. Chouchani ET, Pell VR, Gaude E, Aksentijević D, Sundier SY, Robb EL, Logan A, Nadtochiy SM, Ord ENJ, Smith AC, Eyassu F, Shirley R, Hu CH, Dare AJ, James AM, Rogatti S, Hartley RC, Eaton S, Costa ASH, Brookes PS, Davidson SM, Duchen MR, Kourosh SP, Shattock MJ, Robinson AJ, Work LM, Frezza C, Krieg T, Murphy MP (2014) Ischaemic accumulation of succinate controls reperfusion injury through mitochondrial ROS. Nature 515:431–435. https://doi.org/10.1038/nature13909
9. Chu M, Novak SM, Cover C, Wang AA, Chinyereir Juneman EB, Zarnescu DC, Wong PK, Gregorio CC (2018) Increased cardiac arrhythmogenesis associated with gap junction remodeling with upregulation of RNA-binding protein FXR1. Circulation 137:605–618. https://doi.org/10.1161/CIRCULATIONAHA.117.028976
10. de Diego C, Pai RK, Chen F, Xie LH, De Leeuw J, Weiss JN, Valderrábano M (2008) Electrophysiological consequences of acute regional ischemia/reperfusion in neonatal rat ventricular myocyte monolayers. Circulation 118:2330–2337. https://doi.org/10.1161/CIRCULATIONAHA.108.789149
11. De Nicola GF, Martin ED, Chaikuad A, Bassi R, Clark J, Martino L, Verma S, Sicard P, Tata R, Atkinson RA, Knapp S, Conte MR, Marber MS (2013) Mechanism and consequence of the autoactivation of p38alpha mitogen-activated protein kinase promoted by TAB 1. Nat Struct Mol Biol 20:1182–1190. https://doi.org/10.1038/nsmb.2668
12. Decrock E, Vinken M, De Vuyst E, Krysko DV, D'Herde K, Vanhaecke T, Vandenabeele P, Rogiers V, Leybaert L (2009) Connexin-related signaling in cell death: to live or let die? Cell Death Differ 16:524–536. https://doi.org/10.1038/cdd.2008.196
13. Dunn CA, Lampe PD (2014) Injury-triggered Akt phosphorylation of Cx43: a ZO-1-driven molecular switch that regulates gap junction size. J Cell Biol 127:455–464. https://doi.org/10.1242/jcs.142497
14. Elgenaidi IS, Spiers JP (2019) Regulation of the phosphoprotein phosphatase 2A system and its modulation during oxidative stress: a potential therapeutic target? Pharmacol Ther. https://doi.org/10.1016/j.pharmthera.2019.02.011
15. Eltzschig HK, Eckle T (2011) Ischemia and reperfusion-from mechanism to translation. Nat Med 17:1391–1401. https://doi.org/10.1038/nm.2507
16. Engel FB, Hsieh PC, Lee RT, Keating MT (2006) FGF1/p38 MAP kinase inhibitor therapy induces cardiomyocyte mitosis, reduces scarring, and rescues function after myocardial infarction. Proc Natl Acad Sci USA 103:15546–15551. https://doi.org/10.1073/pnas.0607382
17. Fan GC, Ren X, Qian J, Yuan Q, Nicolaou P, Wang Y, Jones WK, Chu G, Kranias EG (2005) Novel cardioprotective role of a small heat-shock protein, Hsp20, against ischemia/reperfusion injury. Circulation 111:1792–1799. https://doi.org/10.1161/01.CIR.0000160851.41872.C6
18. Garcia-Dorado D, Inserte J, Ruiz-Meana M, Gonzales MA, Solares J, Julia M, Barrabes JA, Soler-Soler J (1997) Gap junction uncoupler heptanol prevents cell-to-cell progression of hypercontracture and limits necrosis during myocardial reperfusion. Circulation 96:3579–3586
19. Glukhov AV, Fedorov VV, Kalish PW, Ravikumar VK, Lou Q, Janks D, Schuessler RB, Moazami N, Efimov IR (2012) Conduction remodeling in human end-stage non-ischemic left ventricular cardiomyopathy. Circulation 125:1835–1847. https://doi.org/10.1161/CIRCULATIONAHA.111.047274
20. Heinzel FR, Luo Y, Li X, Boengler K, Buechert A, García-Dorado D, Di Lisa F, Schulz R, Heusch G (2005) Impairment of diazoxide-induced formation of reactive oxygen species and loss of cardioprotection in connexin 43 deficient mice. Circ Res 97:583–586. https://doi.org/10.1161/01.RES.0000181171.65293.65
21. Hood AR, Ai X, Pogwizd SM (2017) Regulation of cardiac gap junctions by protein phosphatases. J Mol Cell Cardiol 107:52–57. https://doi.org/10.1016/j.yjmcc.2017.05.002
22. Hsu PL, Su BC, Kuok QY, Mo FE (2013) Extracellular matrix protein CCN1 regulates cardiomyocyte apoptosis in mice with stress-induced cardiac injury. Cardiovasc Res 98:64–72. https://doi.org/10.1093/cvr/cvt001
23. Jeyaraman M, Tanguy S, Fandrich RR, Lukas A, Kardami E (2003) Ischemia-induced dephosphorylation of cardiomyocyte connexin-43 is reduced by okadaic acid and calyculin A but not fostriecin. Mol Cell Biochem 242:129–134
24. Jeyaraman MM, Srisakuldee W, Nicke BE, Kardami E (2012) Connexin43 phosphorylation and cytoprotection in the heart. Biochimica et Biophysica Acta 18:2009–2013. https://doi.org/10.1016/j.bbamem.2011.06.023
25. Kang M, Na Lin, Chen Li, Meng Q, Zheng Y, Yan X, Deng J, Ou Y, Zhang C, He J, Luo D (2014) Cx43 phosphorylation on S279/282 and intercellular communication are regulated by IP_3/IP_3 receptor signaling. Cell Commun Signal 12:58. https://doi.org/10.1186/s12964-014-0058-6
26. Koyama T, Temma K, Akera T (1991) Reperfusion-induced contracture develops with a decreasing $[Ca^{2+}]_i$ in single heart cells. Am J Physiol 261:H1115–H1122. https://doi.org/10.1152/ajpheart.1991.261.4.H1115
27. Lampe PD, Cooper CD, King TJ, Burt JM (2006) Analysis of Connexin43 phosphorylated at S325, S328 and S330 in normoxic and ischemic heart. J Cell Sci 119:3435–3442. https://doi.org/10.1242/jcs.03089
28. Li X, Heinzel FR, Boengler K, Schulz R, Heusch G (2004) Role of connexin 43 in ischemic preconditioning does not involve intercellular communication through gap junctions. J Mol Cell Cardiol 36:161–163
29. Lübkemeier I, Requardt RP, Lin X, Sasse P, Andrié R, Schrickel JW, Chkourko H, Bukauskas FF, Kim JS, Frank M, Malan D, Zhang J, Wirth A, Dobrowolski R, Mohler PJ, Offermanns S, Fleischmann BK, Delmar M, Willecke K (2013) Deletion of the last five C-terminal amino acid residues of connexin43 leads to lethal ventricular arrhythmias in mice without affecting coupling via gap junction channels. Basic Res Cardiol 108:348. https://doi.org/10.1007/s00395-013-0348-y
30. Luo D, Yang D, Lan X, Li K, Li X, Chen J, Zhang Y, Xiao RP, Han Q, Cheng H (2008) Nuclear Ca^{2+} sparks and waves mediated by IP_3 receptors in neonatal rat cardiomyocytes. Cell Calcium 43:165–174. https://doi.org/10.1016/j.ceca.2007.04.017
31. Maguy A, Le Bouter S, Comtois P, Chartier D, Villeneuve L, Wakili R, Nishida K, Nattel S (2009) Ion channel subunit expression changes in cardiac Purkinje fibers: a potential role in conduction abnormalities associated with congestive heart failure.

Circ Res 104:1113–1122. https://doi.org/10.1161/CIRCRESAHA.108.191809
32. Martin ED, Bassi R, Marber MS (2015) p38 in cardioprotection—are we there yet? Br J Pharmacol 172:2101–2113. https://doi.org/10.1111/bph.12901
33. Miro-Casas E, Ruiz-Meana M, Agullo E, Stahlhofen S, Rodríguez-Sinovas A, Cabestrero A, Jorge I, Torre I, Vazquez J, Boengler K, Schulz R, Heusch G, Garcia-Dorado D (2009) Connexin43 in cardiomyocyte mitochondria contributes to mitochondrial potassium uptake. Cardiovasc Res 83:747–756. https://doi.org/10.1093/cvr/cvp157
34. Miura T, Ohnuma Y, Kuno A, Tanno M, Ichikawa Y, Nakamura Y, Yano T, Miki T, Sakamoto J, Shimamoto K (2004) Protective role of gap junctions in preconditioning against myocardial infarction. Am J Physiol Heart Circ Physiol 286:H214–H221. https://doi.org/10.1152/ajpheart.00441.2003
35. Mollenhauer M, Friedrichs K, Lange M, Gesenberg J, Remane L, Kerkenpaβ C, Krause J, Schneider J, Ravekes T, Maass M, Halbach M, Peinkofer G, Saric T, Mehrkens D, Adam M, Deuschl FG, Lau D, Geertz B, Manchanda K, Eschenhagen T, Kubala L, Rudolph TK, Wu Y, Tang WHW, Hazen SL, Baldus S, Klinke A, Rudolph V (2017) Myeloperoxidase mediates postischemic arrhythmogenic ventricular remodeling. Circ Res 121:56–70. https://doi.org/10.1161/CIRCRESAHA.117.310870
36. Morel S, Christoffersen C, Axelsen LN, Montecucco F, Rochemont V, Fria MA, Mach F, James RW, Naus CC, Chanson M, Lampe PD, Nielsen MS, Nielsen LB, Kwak BR (2016) Sphingosine-1-phosphate reduces ischaemia-reperfusion injury by phosphorylating the gap junction protein Connexin43. Cardiovasc Res 109:385–396. https://doi.org/10.1093/cvr/cvw004
37. O'Quinn MP, Palatinus JA, Harris BS, Hewett KW, Gourdie RG (2011) A peptide mimetic of the connexin43 carboxyl terminus reduces gap junction remodeling and induced arrhythmia following ventricular injury. Circ Res 108:704–715. https://doi.org/10.1161/CIRCRESAHA.110.235747
38. Porras A, Zuluaga S, Black E, Valladares A, Alvarez AM, Ambrosino C, Benito M, Nebreda AR (2004) p38-mitogen-activated protein kinase sensitizes cells to apoptosis induced by different stimuli. Mol Biol Cell 15:922–933. https://doi.org/10.1091/mbc.E03-08-0592
39. Remo BF, Qu J, Volpicelli FM, Giovannone S, Shin D, Lader J, Liu FY, Zhang J, Lent DS, Morley GE, Fishman GI (2011) Phosphatase-resistant gap junctions inhibit pathological remodeling and prevent arrhythmias. Circ Res 108:1459–1466. https://doi.org/10.1161/CIRCRESAHA.111.244046
40. Rose BA, Force T, Wang Y (2010) Mitogen-activated protein kinase signaling in the heart: angels versus demons in a heartbreaking tale. Physiol Rev 90:1507–1546. https://doi.org/10.1152/physrev.00054.2009
41. Ruiz-Meana M, Rodríguez-Sinovas A, Cabestrero A, Boengler K, Heusch G, Garcia-Dorado D (2008) Mitochondrial connexin43 as a new player in the pathophysiology of myocardial ischaemia–reperfusion injury. Cardiovasc Res 77:325–333. https://doi.org/10.1093/cvr/cvm062
42. Saliba Y, Mougenot N, Jacquet A, Atassi F, Hatem S, Farès N, Lompré AM (2012) A new method of ultrasonic nonviral gene delivery to the adult myocardium. J Mol Cell Cardiol 53:801–808. https://doi.org/10.1016/j.yjmcc.2012.07.016
43. Schreiber T, Salhöfer L, Quinting T, Fandrey J (2019) Things get broken: the hypoxia-inducible factor prolyl hydroxylases in ischemic heart disease. Basic Res Cardiol 114:16. https://doi.org/10.1007/s00395-019-0725-2
44. Schrickel JW, Lickfett L, Lewalter T, Tiemann K, Nickenig G, Baba H, Heusch G, Schulz R, Levkau B (2012) Cardiomyocyte-specific deletion of survivin causes global cardiac conduction defects. Basic Res Cardiol 107:299. https://doi.org/10.1007/s00395-012-0299-8
45. Schulz R, Görge PM, Görbe A, Ferdinandy P, Lampe PD, Leybaert L (2015) Connexin43 is an emerging therapeutic target in ischemia/reperfusion injury, cardioprotection and neuroprotection. Pharmacol Ther 153:90–106. https://doi.org/10.1016/j.pharmthera.2015.06.005
46. Schulz R, Gres P, Skyschally A, Duschin A, Belosjorow S, Konietzka I, Heusch G (2003) Ischemic preconditioning preserves connexin 43 phosphorylation during sustained ischemia in pig hearts in vivo. FASEB J 17:1355–1357
47. Skyschally A, Walter B, Schultz R, Heusch G (2013) The antiarrhythmic dipeptide ZP1609 (danegaptide) when given at reperfusion reduces myocardial infarct size in pigs. Naunyn-Schmiedeberg's Arch Pharmacol 386:383–391. https://doi.org/10.1007/s00210-013-0840-9
48. Smyth JW, Hong TT, Gao D, Vogan JM, Jensen BC, Fong TS, Simpson PC, Stainier DY, Chi NC, Shaw RM (2010) Limited forward trafficking of connexin 43 reduces cell-cell coupling in stressed human and mouse myocardium. J Clin Invest 120:266–279. https://doi.org/10.1172/JCI39740
49. Solan JL, Lampe PD (2009) Connexin43 phosphorylation: structural changes and biological effects. Biochem J 419:261–272. https://doi.org/10.1042/BJ20082319
50. Solan JL, Lampe PD (2018) Spatio-temporal regulation of connexin43 phosphorylation and gap junction dynamics. Biochim Biophys Acta Biomembr 1860:83–90. https://doi.org/10.1016/j.bbamem.2017.04.008
51. Solan JL, Marquez-Rosado L, Sorgen PL, Thornton PJ, Gafken PR, Lampe PD (2007) Phosphorylation of Cx43 at S365 is a gatekeeper event that changes the structure of Cx43 and prevents downregulation by PKC. J Cell Biol 179:1301–1309. https://doi.org/10.1083/jcb.200707060
52. Srisakuldee W, Jeyaraman MM, Nickel BE, Tanguy S, Jiang ZS, Kardami E (2009) Phosphorylation of connexin43 at serine 262 promotes a cardiac injury-resistant state. Cardiovasc Res 83:672–681. https://doi.org/10.1093/cvr/cvp142
53. Sun Z, Yang Y, Wu L, Talabieke S, You H, Zheng Y, Luo D (2019) Connexin 43-serine 282 modulates serine 279 phosphorylation in cardiomyocytes. Biochem Biophys Res Commun 513:567–572. https://doi.org/10.1016/j.bbrc.2019.04.032
54. Tribulová N, Knezl V, Okruhlicová L, Slezák J (2008) Myocardial gap junctions: targets for novel approaches in the prevention of life-threatening cardiac arrhythmias. Physiol Res 57(Suppl 2):S1–S13
55. Wang N, De Vuyst E, Ponsaerts R, Boengler K, Palacios-Prado N, Wauman J, Lai CP, De Bock M, Decrock E, Bol M, Vinken M, Rogiers V, Tavernier J, Evans WH, Naus CC, Bukauskas FF, Sipido KR, Heusch G, Schulz R, Bultynck G, Leybaert L (2013) Selective inhibition of Cx43 hemichannels by Gap19 and its impact on myocardial ischemia/reperfusion injury. Basic Res Cardiol 108:309. https://doi.org/10.1007/s00395-012-0309-x
56. Weinbrenner C, Baines CP, Liu GD, Armstrong SC, Ganote CE, Walsh AH, Honkanen RE, Cohen MV, Downey JM (1998) Fostriecin, an inhibitor of protein phosphatase 2A, limits myocardial infarct size even when administered after onset of ischemia. Circulation 98:899–905. https://doi.org/10.1161/01.CIR.96.10.3579
57. Yang Y, Yan X, Xue J, Zheng Y, Chen M, Sun Z, Liu T, Wang C, You H, Luo D (2019) Connexin43 dephosphorylation at serine 282 is associated with connexin43-mediated cardiomyocyte apoptosis. Cell Death Differ 26:1332–1345. https://doi.org/10.1038/s41418-019-0277-x